Double-analog transition $^{48}Ca(\pi^+,\pi^-)^{48}Ti$ at 35 and 50 MeV

H. W. Baer, M. J. Leitch, R. L. Burman, M. D. Cooper, A. Z. Cui,* B. J. Dropesky, G. C. Giesler, F. Irom, and C. L. Morris
Los Alamos National Laboratory, Los Alamos, New Mexico 87545

J. N. Knudson and J. R. Comfort
Arizona State University, Tempe, Arizona 85287

D. H. Wright
Virginia Polytechnic Institute and State University, Blacksburg, Virginia 24061

R. Gilman
University of Pennsylvania, Philadelphia, Pennsylvania 19104
(Received 21 August 1986)

Differential cross sections for the double-isobaric-analog-state transition in the reaction $^{48}Ca(\pi^+,\pi^-)^{48}Ti$ at an incident energy of 35 MeV were measured over the angular range 20°—80°. The cross section extrapolated to 0° is 3.1 ± 0.8 μb/sr, and the angular distribution shape is nearly isotropic. The results are compared to second-order optical-potential calculations and to the systematics of low-energy double-charge-exchange reactions. Measurements were also made at 50 MeV at scattering angles of 25° and 40°. The analog-state transition could not be clearly observed above the background of non-analog-state transitions.

I. INTRODUCTION

The pion double-charge-exchange (DCX) reaction at low pion energies has gained some interest in recent years because of a surprising experimental result[1,2] on ^{14}C and a novel explanation[3] of this result. The measurements[1,2] on ^{14}C at 50 MeV showed that the differential cross sections of the double isobaric-analog-state (DIAS) transition were unexpectedly large, of order 1 μb/sr at 90°, and that the angular distribution was quite sharply forward peaked, having a 0° cross section of 4 μb/sr. This result was qualitatively explained by Miller[3] by invoking a six-quark cluster probability of 6% in the valence nucleons and by using the chiral-bag model (CBM) to couple the scattered pions to the up and down quarks within a six-quark bag. A similar angular distribution was predicted[4] for ^{18}O, and experiments[5] have verified that ^{18}O and ^{14}C have quite similar cross sections. Several alternative calculations have now been performed, based on the Δ-hole model,[6] second-order optical potentials,[7–9] and a fixed-nucleon multiple-scattering model.[10] All of these models give a fair description of the ^{14}C data. The implications of the various theoretical calculations regarding the range of two-nucleon correlations involved in the double-charge-exchange scattering is still a matter of controversy.

A unique feature of low-energy pion charge exchange is that the angular distribution of the elementary charge-exchange reaction, $\pi^-p\rightarrow\pi^0n$, has a minimum at forward angles for energies near 50 MeV. At 50 MeV the 0° cross section nearly vanishes because of an almost exact cancellation of the s- and p-wave amplitudes. This feature of the elementary reaction is retained in nuclear scattering[11] to isobaric analog states (IAS's). Consequently, for DCX reactions in this energy region the sequential double-forward-scattering amplitude is exceedingly small.[3,10] The forward-angle DCX cross section, if large, must therefore arise from sequential large-angle scatterings, or perhaps from new types of short-range mechanisms. This feature differs from DCX reactions at higher energies (>100 MeV) where the 0° DIAS cross sections are believed[10] to arise predominantly from two forward-angle single-charge-exchange scatterings.

At present, angular distributions have been measured at 50 MeV on the $T=1$ nuclei ^{14}C, ^{18}O, and ^{26}Mg (Ref. 12). They are found to be nearly identical. The 0° cross section in each case is near 4 μb/sr. Since the variation in atomic mass A is nearly a factor of 2 between ^{14}C and ^{26}Mg, there would appear to be only a weak A dependence in the low-energy DIAS cross sections. This result is consistent with an early prediction for DIAS cross sections in light nuclei by Koltun and Reitan,[13]

$$\frac{d\sigma}{d\Omega}\simeq 7.6\frac{q'}{q}\frac{(N-Z)(N-Z-1)}{2}\ (\mu\text{b/sr})\ ,$$

where q and q' are the initial and final pion momenta. This expression results from a plane-wave calculation in which only an s-wave pion-nucleon interaction is assumed. Because the inelasticities of DIAS transitions in light nuclei are small ($q\simeq q'$), this formula gives a low-energy cross section of 7.6 μb/sr for $T=1$ nuclei, which is within a factor of 2 of the values measured. For the ^{48}Ca DIAS transition at an incident energy of 50 MeV, the inelasticity q'/q is equal to 0.8. There is an additional reduction factor of 0.6 between ^{14}C and ^{48}C, arising from the variation in the expectation value of the operator $1/r_{12}$, where r_{12} is the distance between two nucleons.

Including these two factors in the above formula gives a value of approximately 100 μb/sr for ^{48}Ca. Thus, based on the success of this model for nuclei ^{14}C, ^{18}O, and ^{26}Mg, we might have expected a quite large DIAS cross section at low energies for ^{48}Ca.

In addition to the expectation of a large DIAS cross section, ^{48}Ca would seem to be a good nucleus for study because of its excellent closed-shell character.[14] Previous studies have shown that the eight valence neutrons exist in a nearly pure $(f_{7/2})^8$ configuration. Therefore, the DIAS transition must result predominantly from converting two $1f_{7/2}$ neutrons to two $1f_{7/2}$ protons. In a picture of sequential double-charge-exchange scattering, intermediate states are limited to configurations $[f_{7/2}(\text{proton}) \times f^{-1}_{7/2}(\text{neutron})]_J$ with $J=0$—7. All other configurations will have vanishing matrix elements for the second scattering, because they cannot produce the $[f^2_{7/2}(\text{proton}) f^6_{7/2}(\text{neutron})]_{J=0}$ configuration of the DIAS. Thus the nuclear structure aspect is simplified to its most elementary form, charge transfer within a single orbital, and thereby allows theoretical analyses to concentrate on the mechanism of the double charge transfer.

An additional consideration in the choice of ^{48}Ca for this study was the availability of the single-charge-exchange data[15] on ^{48}Ca at 50 MeV. Experience from the ^{14}C study[3,6,7–10] showed that the requirement of describing both the IAS and DIAS cross sections puts much tighter constraints on the theoretical models, which in turn should lead to a less ambiguous interpretation of the DCX reaction mechanism.

The cross sections we report are for an incident beam energy of 35 MeV. We attempted to measure the DIAS cross sections at 50 MeV, but we were not able to observe clearly the DIAS signal above the background of non-analog-state transitions. Upper limits on these differential cross sections are given.

II. EXPERIMENTAL PROCEDURES

The experiment was performed at the low-energy pion (LEP) channel of LAMPF with the new Clamshell spectrometer. A schematic diagram is shown in Fig. 1. This spectrometer has a single dipole with nonparallel pole faces and a flight path of about 2 m. It has a solid angle of approximately 40 msr, a best resolution of several hundred keV, and can measure up to a maximum pion momentum of 260 MeV/c. A trigger is provided by a coincidence of one or more focal-plane scintillators ($S2$,$S3$,$S4$) and a scintillator ($S1$) at the spectrometer entrance. Two x-y drift chambers[16] in the focal plane provide the position and angle in both x and y at the focal plane; these are used to construct the momentum of each particle.

The DCX capability of the Clamshell rests upon the rejection of background events with low pulse height in $S2$ and $S3$ (electrons primarily), the selection of proper time of flight (TOF) between $S1$ and $S2$ (rejection of muons and any electrons surviving the previous criterion), and the observation of a large pulse height in the thick (15 cm) scintillator $S4$ that stops pions up to 70 MeV. The summed analog signal $S=\sum_1^4 S_i$ provides a total energy determination of a pion. Another energy determination is obtained from the momentum analysis by assuming a mass equal to that of the pion. The difference of these two energies (ΔE) vs TOF between S_1 and S_2 is shown in Fig. 2 for π^--^{12}C elastic scattering and the DCX reaction ^{48}Ca(π^+,π^-) at the same outgoing π^- energy. In the elastic scattering, the π^-, μ^-, and e^- groups are clearly identified. The elastic data are used to set the software cuts for pions as shown in Fig. 2. We observed that the response of S_4 to stopping π^+ or π^- differed in that the π^- produce some large scintillation pulses. We attribute these to π^- capture on nuclei with emission of charged fragments. Thus the π^- gates were set as shown, with the large box set to accept the large pulse-height π^- events.

Our DCX cross sections were measured relative to the π^+ elastic cross sections on ^{12}C. These cross sections have been measured at 30 MeV (Ref. 17) and 40 MeV (Ref. 18). Our reaction energy was 34.2 MeV, and we used the interpolated values $d\sigma/d\Omega_{\text{c.m.}}=3.64\pm0.4$ mb/sr for scattering into a laboratory angle of 40° and 3.72 ± 0.20 mb/sr for 80° to calibrate the spectrometer solid angle and pion flux. The correction factor for pion decay in the spectrometer is computed for each trajectory. The relative pion fluxes were measured by means of a toroidal current monitor through which the primary proton beam passed. The relative acceptance of the Clamshell spectrometer as a function of position on the focal plane was determined by measuring the π^+ elastic scattering yields as a function of the magnetic field strength (ac-

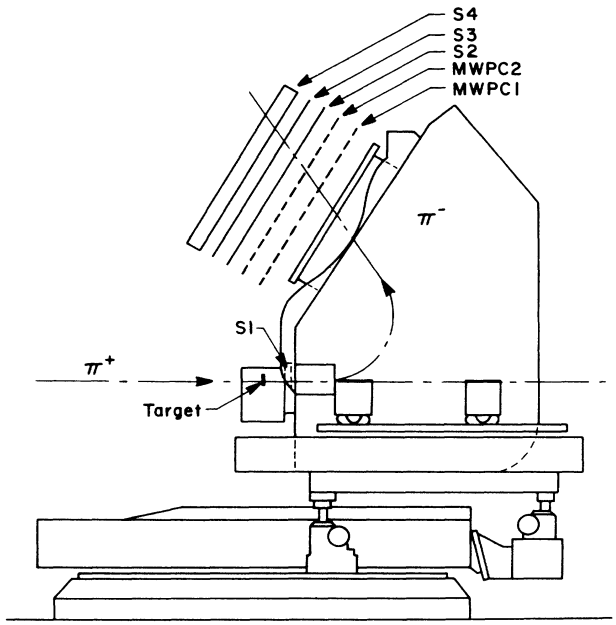

FIG. 1. Elevation view of the Clamshell spectrometer.

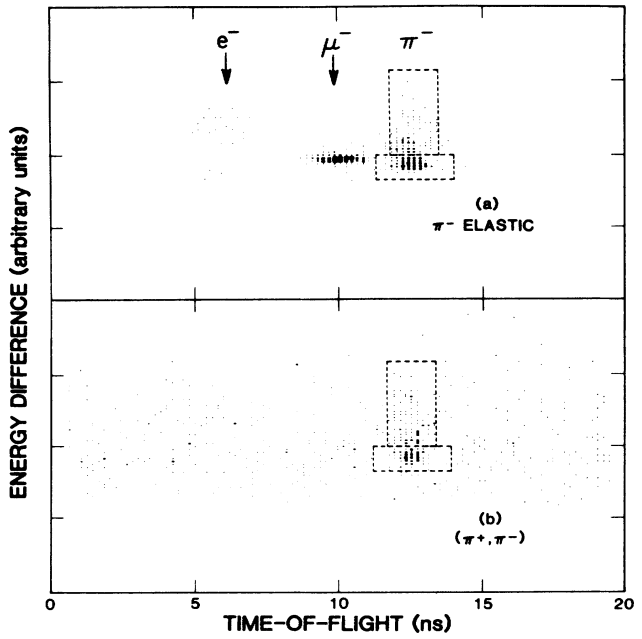

FIG. 2. Particle identification scatter plots for (a) elastic scattering of 22-MeV π^- on ^{12}C at 40° and (b) for 35-MeV DCX on ^{48}Ca at 40°. The plotted variables are energy difference ΔE (defined in the text) vs trajectory-corrected time of flight through the Clamshell magnet.

ceptance scan).

The ^{48}Ca target consisted of a stack of four 3×8 cm plates, each having an areal density of approximately 0.071 g/cm^2. Incident pion fluxes were in the range $(0.5-1)\times10^7$ π^+/s. The incident pion beam energy was 35.0 MeV, and the interaction energy at the center of the target was 34.2 MeV at 40°. We take the latter number to be the average reaction energy for the experiment.

III. RESULTS

Our initial measurements were at a beam energy of 50 MeV. A spectrum measured at 25° is shown in Fig. 3. One can see that there is transition strength to many states, starting at the ^{48}Ti ground state and extending up to 30 MeV, where the spectrometer acceptance falls to zero. The expected position of the DIAS transition is marked by an arrow. A clear signal could not be seen due to a large background of nonanalog transition strength. Upper limits of 3 μb/sr were determined for the DIAS transition at several scattering angles, as given in Table I.

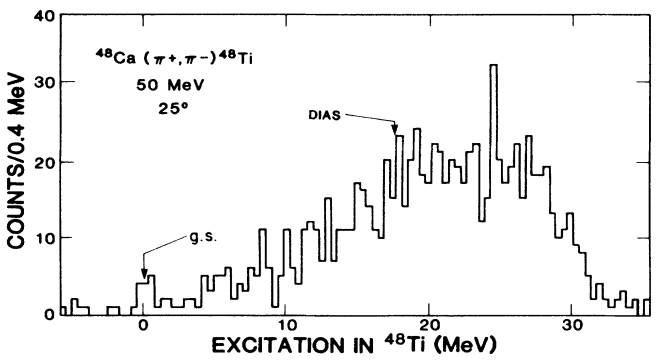

FIG. 3. A spectrum of the $^{48}Ca(\pi^+,\pi^-)$ reaction at 50 MeV.

TABLE I. The measured differential cross section for the $^{48}Ca(\pi^+,\pi^-)^{48}Ti$ (DIAS) reaction.

T_π[a] (MeV)	$\theta_{c.m.}$ (deg)	$d\sigma/d\Omega_{c.m.}$[b] (μb/sr)
34.2	25.1	2.7±0.9
34.2	40.2	2.4±0.7
34.2	80.3	2.2±0.5
49.1	25.2	<3
49.1	40.3	<3

[a]Laboratory kinetic energy at the center of the target.
[b]The errors are relative; they do not include the 10% normalization error.

Spectra measured for the $^{48}Ca(\pi^+,\pi^-)$ reaction at 34.2 MeV are shown in Fig. 4. Compared to the 50-MeV data, there is a dramatic enhancement of the DIAS relative to nonanalog transition strengths. The identification of the DIAS state is based on observation of a peak at the proper reaction Q value. The expected Q value is

$$Q_{\mathrm{DIAS}}(\pi^+,\pi^-) = -\Delta E_C(^{48}\mathrm{Ca}) - \Delta E_C(^{48}\mathrm{Sc}) + 2\Delta_{\mathrm{np}}$$

where $\Delta E_C(Z)$ represents the Coulomb displacement energy for a nucleus with atomic number Z, and $\Delta_{\mathrm{np}}=1.293$ MeV is the neutron-proton mass difference. The Coulomb displacement energies[19] are $\Delta E_C(^{48}Ca)=7.19$ MeV and $\Delta E_C(^{48}Sc)=7.53$ MeV. This gives $Q_{\mathrm{DIAS}}(^{48}Ca)$

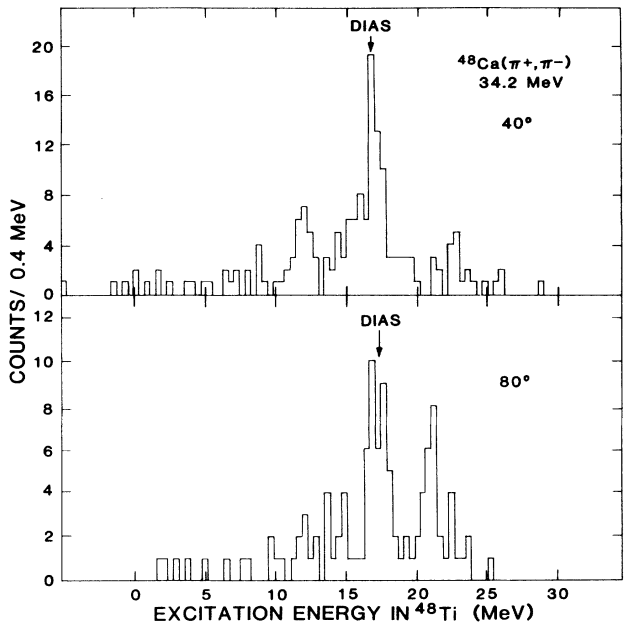

FIG. 4. Spectra for the $^{48}Ca(\pi^+,\pi^-)$ reaction at 34.2 MeV.

$=-12.13$ MeV. The ground state Q value is $Q_{g.s.}(\pi^+,\pi^-)=5.29$ MeV. Therefore the DIAS is expected at an excitation energy of 17.42 MeV in ^{48}Ti, and peaks at this energy are clearly visible in the spectra.

The calibration of the absolute energy scale for the Q-value measurement was made by using 22-MeV π^- elastic scattering on ^{12}C. The Clamshell magnetic field was set as for the ^{48}Ca DCX measurement at 35-MeV incident energy. The outgoing π^- energy for the DIAS was approximately 21 MeV, including energy loss in the target. With this technique, we measured the Q value of the DIAS state to be $-(12.5\pm0.4)$ MeV, in close agreement with the expected value.

The energy resolution with which the DIAS state was measured at 40° was approximately 1.5 MeV full width at half maximum (FWHM). The incident beam energy spread was 0.8 MeV full width (FW), and the ionization straggling was about 0.8 MeV (FWHM). The multiple scattering of the outgoing π^- in the $S1$ scintillator gave a calculated contribution for 21-MeV π's of 0.5 MeV. The vertical beam-spot size of 1.6 cm (FW) gave a contribution of approximately 0.3 MeV. These calculated contributions added in quadrature give 1.6 MeV.

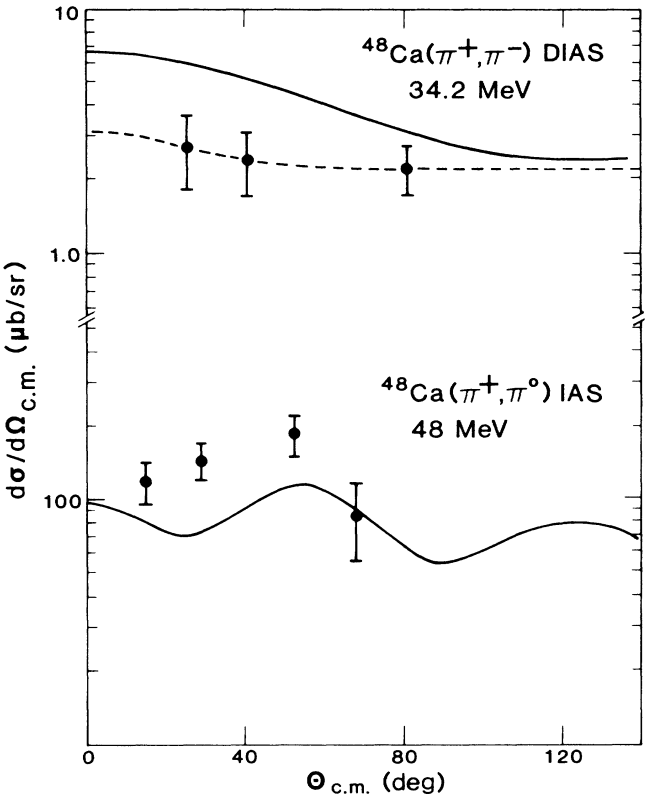

FIG. 5. Top: The angular distribution for the ^{48}Ca(π^+,π^-)^{48}Ti (DIAS) reaction at 34.2 MeV. The dashed line represents the function $B+A\exp[\lambda(\cos\theta-1)]$. The solid curve is a second-order optical model calculation as discussed in the text. Bottom: The angular distribution for the ^{48}Ca(π^+,π^0)^{48}Sc (IAS) reaction at 48 MeV as reported in Ref. 15. The curve is a second-order optical potential calculation using the same parameters as for the DIAS calculation shown in the top panel.

The measured cross sections are listed in Table I and are graphed in Fig. 5. The quoted errors are the relative uncertainties that are dominated by the statistical errors. There is an overall normalization error of 10% arising from uncertainty in the ^{48}Ca target thickness.

To extrapolate the cross sections to 0°, we used the function $B+A\exp[\lambda(\cos\theta-1)]$ that was found to give good representation of the 50-MeV data.[2,5] For this ^{48}Ca data, it gives a 0° differential cross section of 3.1 ± 0.8 μb/sr and an angle-integrated cross section $\sigma_{DIAS}=29\pm9$ μb (dashed curve, Fig. 5).

IV. DISCUSSION

We see that the measured differential cross sections fall far below the 100 μb/sr expected from the plane-wave formula of Koltun and Reitan. Instead of observing the factor $(N-Z)(N-Z-1)$, which would yield a 28-fold increase in the 0° cross section between ^{14}C and ^{48}Ca, we observe a factor close to $(N-Z)(N-Z-1)A^{-10/3}$, as expected from a strong absorption picture.[20] The latter factor would give a 0° value of 1.8 μb/sr for the ^{48}Ca cross section at 49.2 MeV. Such a strong A dependence characterizes the data at 164 and 292 MeV, but was not expected at low energies because the ^{14}C, ^{18}O, and ^{26}Mg data at 50 MeV are nearly A independent.

The forward-angle differential cross sections for the DIAS transitions in ^{14}C, ^{18}O, ^{26}Mg, and ^{48}Ca are shown in Fig. 6. The data points are either 0° or 5° cross sections depending on which angle the cross sections were measured. The ^{14}C, ^{18}O, and ^{26}Mg data show quite similar low-energy behavior, viz., a large rise in cross section as the energy drops from 100 to 50 MeV. For ^{48}Ca the rise still exists, but is less pronounced.

We see that in going from $A=26$ to $A=48$ some new physical effects enter the DCX reaction at low energies and these have the effect of depressing the DIAS cross section and quenching the $(N-Z)(N-Z-1)$ factor associated with the increased number of valence neutrons. Various identifiable differences are the more negative Q value, $Q(^{48}\text{Ca})=-12.2$ MeV vs $Q(^{26}\text{Mg})=-8.0$ MeV; a larger role of the Coulomb force in the incoming and outgoing pion waves, $Z=20$ vs $Z=12$; a higher excitation energy in the residual nucleus, $E_x(^{48}\text{Ti})=-17.4$ MeV vs $E_x{}^{26}(\text{Si})=0$ MeV; and strong distortion of pion waves and absorption of pions in heavy nuclei. We now discuss how these differences might influence the DIAS cross sections.

A more negative Q value gives a larger inelasticity to the reaction. Accordingly, a more substantial reduction factor q'/q would enter into the plane-wave formula of Koltun and Reitan.[13] The cross section for ^{48}Ca would be reduced by a factor of 0.8 to ^{26}Mg, a small effect. The role of the Coulomb force also is expected to be small. Miller and Spencer[24] obtained nearly identical DIAS cross sections for ^{88}Sr at 50 MeV in calculations with and without inclusion of the Coulomb force. From this result, we expect differences between ^{26}Mg and ^{48}Ca that are due to differences in the Coulomb force to be small at 50 and 35 MeV.

The high excitation energy of the DIAS state for ^{48}Ca is a significant difference from the lighter nuclei. However, the effect on the DIAS cross section is not clear. It is plausible to think that this high excitation energy could lead to fragmentation of the double-charge-exchange strength. For example, there are many states at low excitation energies in ^{48}Ti containing configurations of type $f^6_{7/2}(\text{neutron})\times f^2_{7/2}(\text{proton})$. These may be populated in a second scattering from a $f^7_{7/2}(\text{neutron})\times f_{7/2}(\text{proton})$ configuration in the intermediate state, thereby depleting DIAS transition strength. A detailed calculation would be needed in order to give a quantitative estimate of this effect.

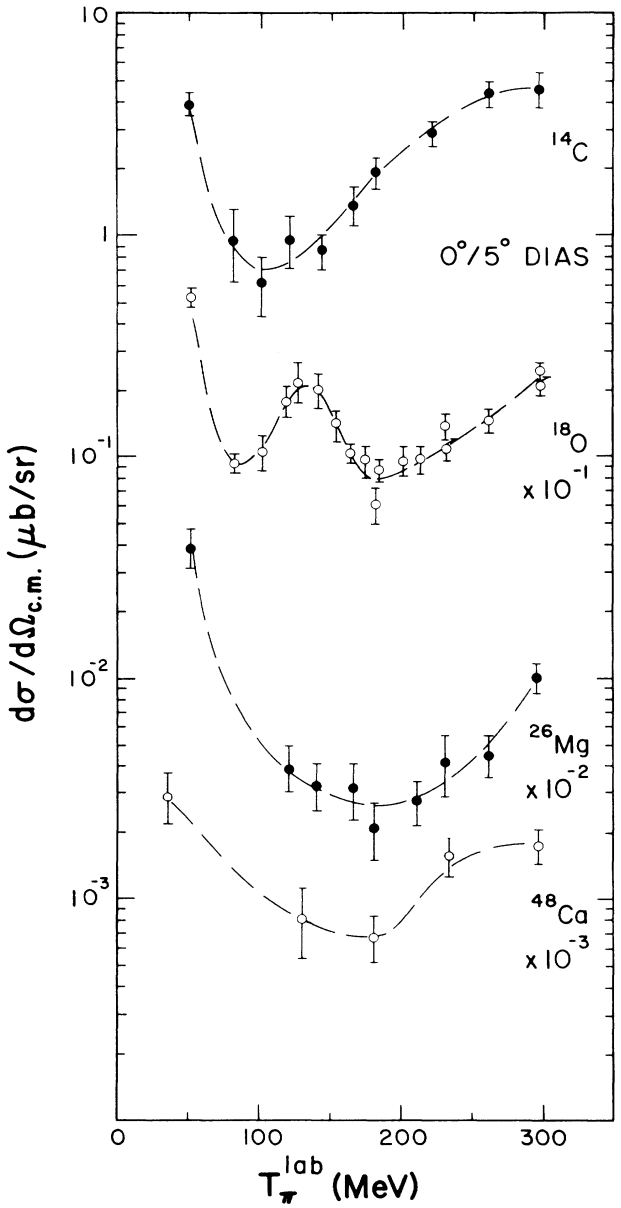

FIG. 6. Excitation functions at 0° or 5° for the DIAS transitions in ^{14}C, ^{18}O, ^{26}Mg, and ^{48}Ca. Data are taken from Refs. 2, 5, 12, 21–23, and the present work.

TABLE II. Parameters used in the PIESDEX calculations for the $^{48}Ca(\pi^+,\pi^-)^{48}Ti$ (DIAS) transition at 34.2 MeV. The definitions follow Ref. 8.

First order isoscalar (U_0):	$\lambda^{(1)}_{s0}=(-2.39+0.22i)$ fm^3
	$\lambda^{(1)}_{p0}=(8.40+0.37i)$ fm^3
First order isovector (U_1):	$\lambda^{(1)}_{s1}=(-9.12+0.15i)$ fm^3
	$\lambda^{(1)}_{p1}=(10.91+0.30i)$ fm^3
Second order isoscalar (U_0):	$\lambda^{(2)}_{s0}=(-0.11+0.74i)$ fm^3
	$\lambda^{(2)}_{p0}=(0.67+1.09i)$ fm^3
Second order isovector (U_1):	$\lambda^{(2)}_{s1}=0$
	$\lambda^{(2)}_{p1}=(0.0-1.0i)$ fm^3
Second order isotensor (U_2):	$\lambda^{(2)}_{s2}=0$
	$\lambda^{(2)}_{p2}=(1.7+0.0i)$ fm^3
Pauli factor:	$=0.21$
EL correlation (α):[a]	$=1.6$

[a]Extended Lorentz-Lorentz effect as defined in Ref. 8.

A possibly large effect would seem to be in the distortion of the pion waves and in the absorption of pions by the nucleus. We investigated these with second-order optical model calculations performed with the code PIESDEX.[7,8] The general form of the optical potential employed is

$$U=U_0+U_1(\mathbf{t}_\pi\cdot\mathbf{T})+U_2(\mathbf{t}_\pi\cdot\mathbf{T})^2 .$$

We show in Fig. 5 calculations based on this form of the potential and with the parameters used in Refs. 7, 8, and 15 to fit 50 MeV single- and double-charge exchange data. The transition density was taken to be $\Delta\rho=(N-Z)\rho_0$, where ρ_0 is a three-parameter Fermi function as determined from electron scattering (Ref. 25). The parameters of our calculation are listed in Table II. The earlier studies of IAS transitions in ^{14}C, ^{15}N, ^{39}K, and ^{48}Ca showed that it was necessary to include second-order terms in U_1 to describe the data. In particular, a second-order isovector p-wave term $\lambda^{(2)}_{p1}=(0.0-1.0i)$ fm^3 was employed. Use of this value leads to a slight underestimation of the ^{48}Ca IAS cross section at 48 MeV, as shown in Fig. 5. For the DIAS transition, both the iterated operation of the isovector U_1 term and the isotensor U_2 term contribute to the transition amplitude. With the optical potential cast in the form given above, it is only the U_2 term that allows for nonanalog intermediate states. The parameters that govern the U_2 term are not yet well determined. The use of an isotensor p-wave absorption coefficient $\lambda^{(2)}_{p2}=(1.7+0i)$ fm^3 gave[7,8] a good description of the DIAS angular distribution for ^{14}C at 50 MeV. The curve shown with our data on ^{48}Ca at 34.2 MeV was calculated with this value. We see that the calculated cross sections are much less than the plane-wave value of 100 μb/sr.

A systematic study of the energy dependence of the second-order s- and p-wave terms in U_0, U_1, and U_2, based on all available low-energy data is in progress. The representative calculations given here serve primarily to demonstrate the large role played by the absorption terms in reducing the DIAS cross sections from plane-wave values near 100 μb/sr to the experimental values of 1–2 μb/sr.

It is interesting to compare the A dependence of IAS and DIAS transitions at low pion energies. In a recent

study[26] of IAS transitions at 20 MeV on nuclei varying in A from ^{7}Li to ^{120}Sn, it was found that the 0° cross sections are quite well described by $(N-Z)A^{-0.73}$. The angular distribution for ^{7}Li was nearly isotropic. This weakened A dependence, relative to the $A^{-1.33}$ characteristic of strong absorption,[20] is in marked contrast to the strong A dependence we find for the DIAS transition in going from the light nuclei to ^{48}Ca.

V. SUMMARY

Our measurements show that the trends for the low-energy DIAS cross section set by the previous measurements on ^{14}C, ^{18}O, and ^{26}Mg break down for ^{48}Ca. The cross sections are much lower than expected from the large neutron excess of ^{48}Ca. The forward-angle cross sections at 35 MeV for ^{48}Ca relative to ^{14}C follow more nearly the strong absorption formula $(N-Z)(N-Z-1)A^{-10/3}$ than the plane-wave formula, which is independent of A. Various explanations for this effect were examined. The high excitation energy of DIAS states in heavy nuclei and an increased role of pion absorption are identified as possible causes for the reduction of the DIAS cross sections. A quantitative explanation for the small DIAS cross sections in ^{48}Ca must await future theoretical work.

Our experiment reports a new effect in low-energy DCX reactions. There is a dramatic improvement in the signal-to-background ratio for the DIAS transition as the incident energy is lowered from 50 to 35 MeV. This is useful to know for planning future experiments, and its implications for DCX reaction dynamics should be investigated.

From our results, a future line of experimentation for the DIAS transition is suggested. The trend of A independence for $T=1$ nuclei should be investigated further on ^{30}Si, ^{34}S, and ^{42}Ca to characterize the onset of the DCX suppression mechanism. The dependence on $(N-Z)(N-Z-1)$, and the effect of higher excitation energies for the DIAS state, can be tested by comparison of ^{42,44,48}Ca. The availability of these data would seem to be essential for a quantitative understanding of the double-charge-exchange process in heavy nuclei.

ACKNOWLEDGMENTS

We thank R. Boudrie for assistance with the installation and operation of the Clamshell spectrometer. This work was supported by the U.S. Department of Energy and in part by the National Science Foundation.

*Permanent address: Institute for Atomic Energy, Beijing, People's Republic of China.

[1] I. Navon, M. J. Leitch, D. A. Bryman, T. Numao, P. Schlatter, G. Azuelos, R. Poutissou, R. A. Burnham, M. Hasinoff, J. M. Poutissou, J. A. MacDonald, J. E. Spuller, C. K. Hargrove, H. Mes, M. Blecher, K. Gotow, M. Moinester, and H. W. Baer, Phys. Rev. Lett. **52**, 105 (1984).

[2] M. J. Leitch, E. Piasetzky, H. W. Baer, J. D. Bowman, R. L. Burman, B. J. Dropesky, P. A. M. Gram, F. Irom, D. Roberts, G. A. Rebka, Jr., J. N. Knudson, J. R. Comfort, V. A. Pinnick, D. H. Wright, and S. A. Wood, Phys. Rev. Lett. **54**, 1482 (1985).

[3] G. A. Miller, Phys. Rev. Lett. **53**, 2008 (1984).

[4] G. A. Miller, in Proceedings, LAMPF Workshop on Pion Double Charge Exchange (1985), edited by H. W. Baer and M. J. Leitch, Los Alamos National Laboratory Report LA-10550-C, p. 193.

[5] A. Altman, R. R. Johnson, U. Wienands, N. Hessey, B. M. Barnett, B. M. Forster, N. Grion, D. Mills, F. M. Rozon, G. R. Smith, R. P. Trelle, D. R. Gill, G. Sheffer, and T. Anderl, Phys. Rev. Lett. **55**, 1273 (1985).

[6] T. Karapiperis and M. Kobayashi, Phys. Rev. Lett. **54**, 1230 (1985).

[7] E. R. Siciliano, in Ref. 4, p. 179.

[8] E. R. Siciliano, M. D. Cooper, M. B. Johnson, and M. J. Leitch, Phys. Rev. C **34**, 267 (1986).

[9] L. C. Liu, in Ref. 4, p. 109.

[10] W. R. Gibbs, W. B. Kaufmann, and P. B. Siegel, in Ref. 4, p. 90.

[11] F. Irom, M. J. Leitch, H. W. Baer, J. D. Bowman, M. D. Cooper, B. J. Dropesky, E. Piasetzky, and J. N. Knudson, Phys. Rev. Lett. **55**, 1862 (1985).

[12] A. Altman, R. R. Johnson, B. M. Barnett, N. Grion, N. Hessey, D. Mills, F. M. Rozon, G. R. Smith, M. Sevior, R. P. Trelle, V. Wienands, D. R. Gill, G. Sheffer, and T. Anderl, Bull. Am. Phys. Soc. **31**, 802 (1986).

[13] D. S. Koltun and A. Reitan, Phys. Rev. **139**, B1372 (1965).

[14] S. M. Banks, B. M. Spicer, G. G. Shute, V. C. Officer, G. J. Wagner, W. E. Dollhopf, L. Qingli, C. W. Glover, D. W. Devins, and D. L. Friesel, Nucl. Phys. **A437**, 381 (1985); P. Martin, M. Buenerd, Y. Dupont, and M. Chabre, *ibid.* **185**, 465 (1972).

[15] M. J. Leitch, H. W. Baer, J. D. Bowman, M. D. Cooper, E. Piasetzky, U. Sennhauser, H. J. Ziock, F. Irom, P. B. Siegel, and M. A. Moinester, Phys. Rev. C **33**, 278 (1985).

[16] L. G. Atencio, J. F. Amann, R. L. Boudrie, and C. L. Morris, Nucl. Instrum. Methods **187**, 381 (1981).

[17] B. M. Preedom, S. H. Dam, C. W. Darden III, R. D. Edge, D. J. Malbrough, T. Marks, R. L. Burman, M. Hamm, M. A. Moinester, R. P. Redwine, M. A. Yates, F. E. Bertrand, T. P. Cleary, E. E. Gross, N. W. Hill, C. A. Ludemann, M. Blecher, K. Gotow, D. Jenkins, and F. Milder, Phys. Rev. C **23**, 1134 (1981).

[18] M. Blecher, K. Gotow, D. Jenkins, F. Milder, F. E. Bertrand, T. P. Cleary, E. E. Gross, C. A. Ludemann, M. A. Moinester, R. L. Burman, M. Hamm, R. P. Redwine, M. Yates-Williams, S. Dam, C. W. Darden III, R. D. Edge, D. J. Malbrough, T. Marks, and B. M. Preedom, Phys. Rev. C **20**, 1884 (1979).

[19] W. J. Courtney and J. D. Fox, At. Data Nucl. Data Tables **15**, 141 (1975).

[20] M. B. Johnson, Phys. Rev. C **22**, 192 (1980).

[21] P. A. Seidl, M. D. Brown, R. R. Kiziah, C. F. Moore, H. W. Baer, C. L. Morris, G. R. Burleson, W. B. Cottingame, S. J. Greene, L. C. Bland, R. Gilman, and H. T. Fortune, Phys. Rev. C **30**, 973 (1984); R. Gilman, H. T. Fortune, J. D. Zumbro, P. A. Seidl, C. F. Moore, C. L. Morris, J. A. Faucett, G. R. Burleson, S. Mordechai, and K. S. Dhuga, *ibid.* **33**, 1082

(1986).

[22]S. J. Greene, W. J. Braithwaite, D. B. Holtkamp, W. B. Cottingame, C. F. Moore, G. R. Burleson, G. S. Blanpied, A. J. Viescas, G. H. Daw, C. L. Morris, and H. A. Thiessen, Phys. Rev. C **25**, 927 (1982); R. L. Burman, M. P. Baker, M. D. Cooper, R. H. Heffner, D. M. Lee, R. P. Redwine, J. E. Spencer, T. Marks, D. J. Malbrough, B. M. Preedom, R. J. Holt, and B. Zeidman, *ibid.* **17**, 1774 (1978).

[23]M. O. Kaletka, Ph.D. dissertation, Northwestern University, 1983; Los Alamos National Laboratory Report LA-9947-T, 1984 (unpublished).

[24]G. A. Miller and J. E. Spencer, Ann. Phys. (N.Y.) **100**, 562 (1976).

[25]C. W. deJager, H. deVries, and C. deVries, At. Data Nucl. Data Tables **14**, 479 (1974).

[26]F. Irom, H. W. Baer, J. D. Bowman, A. B. Bergman, P. Heusi, D. H. Fitzgerald, C. J. Seftor, M. E. Sadler, K. J. Smith, J. N. Knudson, E. Piasetzky, S. H. Rokni, and W. Biscoe, Bull. Am. Phys. Soc. **31**, 856 (1986).